

CERN-EP/83-148  
27 September 1983

DETERMINATION OF NUCLEAR SPINS AND MOMENTS IN  
A SERIES OF RADIUM ISOTOPES

S.A. Ahmad<sup>1)</sup>, W. Klempt<sup>2)</sup>  
CERN, Geneva, Switzerland

R. Neugart, E.W. Otten, K. Wendt<sup>3)</sup>  
Institut für Physik, Universität Mainz, Fed. Rep. Germany

C. Ekström  
Department of Physics, Chalmers University of Technology,  
Gothenburg, Sweden

and

The ISOLDE Collaboration  
CERN, Geneva, Switzerland

ABSTRACT

The first investigation of hyperfine structure in radium isotopes has enabled the determination of nuclear spins, magnetic dipole and electric quadrupole moments of the isotopes with mass numbers  $A=211, 213, 221, 223, 225, 227$  and  $229$ . Isotope shifts in the mass range  $208 \leq A \leq 232$  have also been measured. These studies were carried out using the technique of on-line collinear fast beam laser spectroscopy.

(Submitted to Phys. Letters B)

- 
- 1) On leave from the Bhabha Atomic Research Centre, Bombay, India.
  - 2) On leave from the Institut für Physik, Mainz, Fed. Rep. Germany.
  - 3) Present address: EP Division, CERN, Geneva, Switzerland.





The radioactive element radium was discovered by Mme. Curie in 1898 and subsequently many short-lived isotopes of Ra have been found. But prior to the present study neither the nuclear spins had been measured directly nor the nuclear moments had been determined for any of the odd-A isotopes. Here we report the first investigation of the hyperfine structure (hfs) and isotope shift (IS) of a series of Ra isotopes with half-lives between 23 msec and 1600 years, using the on-line collinear fast beam laser spectroscopy technique which is described in detail elsewhere[1,2]. The analysis of the hfs has provided the first determination of nuclear spins and moments of seven odd-A isotopes of Ra.

The experiment was carried out at the ISOLDE mass separator [3] at CERN. Spallation of  $^{238}\text{U}$ , induced by 600 MeV protons from the CERN synchro-cyclotron, leads to an efficient production of Ra isotopes. The target ( $12\text{g}/\text{cm}^2$ ) consists of  $\text{UC}_2$  formed at the surface of a graphite cloth. During operation it is heated to  $2200^\circ\text{C}$  in order to release the volatile spallation products. The atoms are surface-ionized on hot ( $2400^\circ\text{C}$ ) tungsten forming the orifice of the target container. After acceleration to 60 KeV they are mass-separated and transmitted to the apparatus. This system gives an efficient release of the alkaline-earth reaction products with half-lives longer than 1 sec. For typical proton-beam intensities of  $2\ \mu\text{A}$ , the yields are between  $10^8$  atoms/sec ( $^{224}\text{Ra}$ ) and  $10^4$  atoms/sec ( $^{208}\text{Ra}$  and  $^{232}\text{Ra}$ ), with a gap in the mass range  $214 < A < 220$  due to the short half-lives of these isotopes ( $1\ \mu\text{s} < T_{1/2} < 1\text{ms}$ ).

The optical-high resolution measurements on 18 Ra isotopes in the range  $208 \leq A \leq 232$  have been carried out in the  $4826\ \text{\AA}$  line ( $7s^2\ ^1S_0 - 7s7p\ ^1P_1$ ) of the neutral Ra and the  $4683\ \text{\AA}$  line ( $7s\ ^2S_{1/2} - 7p\ ^2P_{1/2}$ ) of the  $\text{Ra}^+$  spectra [4]. Both these lines are the strongest resonance lines of the respective systems suitable for laser spectroscopy. A commercial single-frequency dye laser, operated with the dye coumarin 102, was used for the experiment. As an example, the hfs of  $^{223}\text{Ra}$  in the two lines are shown in Fig. 1. The relative positions of all the resonances observed in both the lines have been evaluated with an experimental error of  $< 10\text{MHz}$ . The resonances in the atomic line ( $4826\ \text{\AA}$ ) are plotted in Fig. 2, taking as reference the isotope  $^{214}\text{Ra}$  with the closed neutron shell  $N=126$ .

The hyperfine energy is given by the well-known formula

$$W_{\text{hfs}} = \frac{C}{2} A + \frac{3/4 C(C+1) - J(J+1)I(I+1)}{2J(2J-1)I(2I-1)} B \quad (1)$$

where  $C=F(F+1)-J(J+1)-I(I+1)$ . The electronic angular momentum  $J$  and the nuclear spin  $I$  couple to give the total angular momentum  $F$ .  $A$  and  $B$  are the magnetic dipole and electric quadrupole interaction constants given by  $A=\mu_I H_e(0)/IJ$  and  $B=eQ_S \phi_{zz}$  where  $\mu_I$  is the magnetic dipole and  $Q_S$  the spectroscopic quadrupole moment,  $H_e(0)$  is the magnetic field and  $\phi_{zz}$  the electric field gradient of the valence electrons at the nucleus.

From the hfs splittings of one of the transitions it is not possible to uniquely determine the three relevant hfs parameters  $I$ ,  $A$  and  $B$ . The relative intensities of the hfs components depend, however, on  $I$  through Clebsch-Gordan coefficients and can thus be used to determine the value of  $I$ . But since these intensity ratios are affected by optical pumping dynamics, a comparative study of the hfs splittings in two transitions is preferable. A combined analysis of the hfs in the two lines has provided the first direct measurement of the nuclear spins of Ra isotopes (Table 1). Another, even more important reason for extending the experiments to several spectral lines is the evaluation of  $H_e(0)$  and  $\phi_{zz}$  as well as of the electronic densities  $|\Psi(0)|^2$ . The evaluation of these parameters in the alkali-like one-electron spectrum of the ion is simpler than in the two-electron spectrum of the atom which is affected by the breakdown of the LS-coupling and the mixing of the triplet and the singlet states. Hence, the analysis of the sp-configuration needs more information than just the hfs parameters from only one of its states.

The analysis of the hfs in the atomic and the ionic lines gives the nuclear spins, the A-factors of the  $7s7p \ ^1P_1$ ,  $7s \ ^2S_{1/2}$  and  $7p \ ^2P_{1/2}$  states and the B-factors of the  $7s7p \ ^1P_1$  state, which are presented in Table 1. Since no direct measurement of the nuclear g-factor  $g_I$  has been performed so far for any of the Ra isotopes, the magnetic hyperfine field  $H_e(0)$  can not be calibrated with experimental data. Therefore we rely on a semi-empirical evaluation of  $H_e(0)$  [5]. The hfs interaction in the  $7s \ ^2S_{1/2}$  state is due to the Fermi-contact term and thus the A-factor is connected to  $\mu_I$  by the following relation

$$A_{ns} = \frac{8\pi}{3} |\Psi_{ns}(0)|^2 a_o^3 R_\infty \alpha^2 F_r (1-\delta) (1-\epsilon) \frac{1}{1836.1} \frac{\mu_I}{I \mu_n} \quad (2)$$

where  $|\Psi_{ns}(0)|^2$  is the non-relativistic density of the ns-electron at the nucleus and  $F_r$ ,  $\delta$  and  $\epsilon$  are the correction factors. According to Goudsmit-Fermi-Segrè,  $|\Psi_{ns}(0)|^2$  can be obtained from the effective quantum number  $n_s$  and the quantum defect  $\sigma$  describing the term values in the alkali-like spectrum:  $|\Psi_{ns}(0)|^2 = (Z_i Z_a^2 / \pi a_o^3 n_s^3) (1-d\sigma/dn)$ . For the 7s-electron, we

get  $|\Psi_{7s}(0)|^2 = 10.06a_0^{-3}$ , with  $Z_1=88$ ,  $Z_a=2$  and using  $n_s=2.316$  and  $1-d\sigma/dn=1.115$  evaluated from the data on the spectrum of  $Ra^+$  [4]. The relativistic correction factor  $F_r = 2.90$ , the nuclear volume correction  $(1-\delta) = 0.81$  and the correction for the distribution of the nuclear magnetism  $(1-\epsilon) = 0.96$  have been evaluated using the relations as given in [5].

The  $\mu_I$ -values, obtained using the above values and the relation (2) and applying the diamagnetic correction according to [6], are included in Table 1. The systematic error is estimated to be of the order of 5%, and includes the uncertainty about the hfs anomaly. The ionic ground state hfs anomaly  $\Delta$  between the isotopes  $^{x}Ra$  and  $^{213}Ra$  is given by

$$x_{\Delta}^{213} = \frac{x_A(^{2}S_{1/2})^{213}g_I}{^{213}A(^{2}S_{1/2})x_{g_I}} - 1 \quad (3)$$

in which the ratio of the  $g_I$ -factors can be approximated by the ratio  $x_A(^{2}P_{1/2})/^{213}A(^{2}P_{1/2})$ . The  $x_{\Delta}^{213}$  values, included in table 1, are found to be  $\leq 0.6\%$  which is of the same order as the present experimental error. By inserting into (3)  $A(^{1}P_1)$  instead of  $A(^{2}P_{1/2})$ ,  $\Delta$  reduces, which appears reasonable since  $A(^{1}P_1)$  is expected to have, in the intermediate coupling case, a dominant contribution of the 7s electron, the same as in the ionic ground state.

The  $Q_s$ -values listed in Table 1 have been obtained from the ratio of B-factors measured in the  $7s7p \ ^{1}P_1$  state, using a reference value of  $Q_s=2.9b$  for the strongly-deformed isotope  $^{229}Ra$ . This value has been calculated by applying the strong-coupling projection formula to the intrinsic moment  $Q_0=8.0b$ , as extrapolated from the neighbouring even isotopes [7]. A systematic error  $<15\%$  is expected for this procedure by experience.

Our values of ground state nuclear spins confirm the probable spin assignments [6] for the isotopes  $^{211}Ra$ ,  $^{213}Ra$  and  $^{227}Ra$ , as well as the conclusion from a recent study of  $^{225}Ra$  [8]. The spin assignment of  $^{223}Ra$  [6] has to be revised on the basis of the present study.

The spins and the magnetic moments of the almost spherical nuclei  $^{211}Ra$  and  $^{213}Ra$ , close to the magic neutron number, can be assigned to the neutron shell-model states  $(f_{5/2})^{-1}$  and  $(p_{1/2})^{-1}$ , respectively. In Table 2, they are compared to those of the Hg, Pb and Po isotones as well as to the corresponding Schmidt values. The  $^{213}Ra$  case shows that the  $p_{1/2}$  moment is very close to the Schmidt value. It is known to be quite insensitive to core polarization as well as mesonic effects (compare the discussion in [9] and references therein). This agreement also supports our semi-empirical evaluation of the magnetic moments. The magnetic moments of the  $(f_{5/2})^{-1}$

states are also rather stable but show the usual quenching of  $g_s = 0.6g_{s,free}$  from the Schmidt value. The quadrupole moments of these nuclides reach a minimum for the magic  $^{205}\text{Pb}$  nucleus, whereas for the others the  $Q_s$ -values indicate a slight deformation.

For the neutron-rich odd-A isotopes  $^{221-229}\text{Ra}$ , we have made preliminary calculations of the nuclear dipole and quadrupole moments within the particle-plus-rotor model [12]. The results are given in Fig. 3 as a function of the quadrupole deformation parameter  $\varepsilon$ . The  $A=225$  potential parameters  $\kappa=0.0635$  and  $\mu=0.346$ , and the  $g$ -factors  $g_R=Z/A$ ,  $g_s=0.6g_{s,free}$  and  $g_l=0$  were used in the calculations. No Coriolis attenuation was applied and the hexadecapole deformation parameter  $\varepsilon_4$  was set to zero in this first approach. In Fig. 3, the experimental nuclear moments are placed at the deformations (arrows) derived from the intrinsic quadrupole moments interpolated or extrapolated from the even-A isotopes[7]; the corresponding strong-coupling spectroscopic moments are given by short horizontal lines. As can be seen from the figure, the experimental quadrupole moments gradually approach the strong-coupling limit towards the end of the series, i.e. for large deformations and maximum projection factor, as expected. The agreement with the theoretical prediction is rather satisfying except for  $^{223}\text{Ra}$  where the configuration of the nuclear ground state may have been not properly chosen.

The magnetic moments, however, are only qualitatively reproduced by the present calculation. Generally, better agreement is obtained by the inclusion of a Coriolis attenuation of about 35% and  $\varepsilon_4$ -values between -0.05 and -0.1. On the other hand, the assumption  $g_s = 0.6g_{s,free}$  might be too schematic to give a proper account of the core-polarisation to which quite a number of states inside and outside the particle-plus-rotor model space may contribute. Another interesting explanation comes from the consideration of the influence of static octupole deformation on the theoretical evaluation of the magnetic moments. In two very recent approaches, Ragnarsson [13] and Leander and Sheline [14] have included the octupole degree of freedom into calculations within the Nilsson model and using the folded Yukawa single-particle potential, respectively. These calculations reproduce well the experimental magnetic moments by the assumption of an octupole deformation  $\varepsilon_3=0.1$  for the lighter isotopes and decreasing values for the heavier. This is consistent with predictions from potential-energy calculations [15] and from the excitation energies of the  $0^-$  bands in the neighbouring even-A isotopes.

The IS has been determined in both the atomic and the ionic lines for all the isotopes shown in Fig. 2. The influence of the neutron shell closure on the IS is apparent from the change in the slope at  $N=126$ . The calculation of the mean square nuclear charge radii  $\delta\langle r^2 \rangle$  as well as their

interpretation is under way and will be published separately.

The present study provides the first systematic investigation of nuclear spins and moments in radium. For further strengthening the evaluation of the nuclear moments, we plan to extend these measurements to the triplet states of the atomic  $7s7p$  configuration as well as to the  $7s \ ^2P_{3/2}$  state of the ion.

We are grateful to G. Løvholden for his comments on the importance of clear-cut spin measurements in the heavy radium isotopes, and to I. Ragnarsson and G. Leander for interesting discussions on the octupole deformation in this region and for making available the yet unpublished results of their calculations. This work was supported by the Bundesministerium für Forschung und Technologie and the Deutsche Forschungsgemeinschaft.

#### References

- [1] K.-R. Anton, S.L. Kaufman, W. Klempt, G. Moruzzi, R. Neugart, E.W. Otten and B. Schinzler, Phys. Rev. Lett. 40 (1978) 642.
- [2] A.C. Mueller, F. Buchinger, W. Klempt, E.W. Otten, R. Neugart, C. Ekström and J. Heinemeier, Nucl. Phys. A 403 (1983) 234.
- [3] H.L. Ravn, Phys. Rep. 54 (1979) 201.
- [4] E. Rasmussen, Z. Phys. 87 (1934) 607 and 86 (1933) 24.
- [5] H. Kopfermann, Nuclear Moments (Academic Press, New York), 1958.
- [6] C.M. Lederer and V.S. Shirley, Table of Isotopes, 7<sup>th</sup> ed., (John Wiley & Sons, New York) 1978.
- [7] K.E.G. Löbner, M. Vetter and V. Hönig, Nucl. Data Tables A7 (1970) 495.
- [8] K. Nybø, T.F. Thorsteinsen, G. Løvholden, E.R. Flynn, J.A. Cizewski, R.K. Sheline, D. Decman, D.G. Burke, G. Sletten, P. Hill, N. Kaffrell, W. Kurcewicz and G. Nyman, The nuclear structure of  $^{225}\text{Ra}$ , to be published in Nucl. Phys. A.
- [9] J. Rodriguez, J. Bonn, G. Huber, H.J. Kluge and E.W. Otten, Z. Phys. A 272 (1975) 369.
- [10] R.C. Thompson, M. Anselment, K. Bekk, S. Göring, A. Hanser, G. Meisel, H. Rebel, G. Schatz and B.A. Brown, J. Phys. G 9 (1983) 443.
- [11] P. Herzog, H. Walitzki, K. Freitag, H. Hildebrand and K. Schlösser, Z. Phys. A 311 (1983) 351.
- [12] S.E. Larsson, G. Leander and I. Ragnarsson, Nucl. Phys. A 307 (1978) 189.
- [13] I. Ragnarsson, Further evidence for reflection asymmetry in the Ra region - the decoupling parameter and the magnetic moment, to be published

in Phys. Lett. B.

[14] G.A. Leander and R.K. Sheline, Intrinsic reflection asymmetry in odd-A nuclei, to be published in Nucl. Phys. A.

[15] G.A.Leander, R.K.Sheline, P.Möller, P.Olanders, I.Ragnarsson, and A.J.Sierk, Nucl. Phys. A 388 (1982) 452.



Table 1  
 Hyperfine structure constants, nuclear spins and moments of Ra isotopes. The estimated errors in the  $\mu_I$  and  $Q_S$  values are 5% and 15%, respectively.

Mass number	I	$A(^2S_{1/2})$ (MHz)	$A(^2P_{1/2})$ (MHz)	$A(^1P_1)$ (MHz)	$B(^1P_1)$ (MHz)	$\chi_{\Delta^{213}}$	$\mu_I$ (n.m.)	$Q_S$ (b)
211	5/2	6624.8(1.0)	1299.7(8)	-668.4(9)	162(4)	0.006(2)	0.90	0.45
213	1/2	22920(6)	4525(5)	-2314.8(2.5)			0.62	
221	5/2	-1345.0(1.8)	-266.3(1.5)	136.3(8)	669.6(3.0)	-0.003(8)	-0.18	1.9
223	3/2	3398.3(2.9)	667.1(2.1)	-344.5(9)	421.5(1.6)	0.006(5)	0.28	1.2
225	1/2	-27684(13)	-5446(7)	2796.5(2.5)		0.004(3)	-0.75	
227	3/2	-5063.5(3.1)	-996.2(2.3)	512.5(2.3)	531(5)	0.003(4)	-0.41	1.5
229	5/2	3789.7(2.3)	743.9(1.2)	-382.7(1.4)	1042(5)	0.006(4)	0.51	2.9

Table 2  
Comparison of the magnetic moments  $\mu_I$  (in n.m.) and the electric quadrupole moments  $Q_S$  (in barns) for the isotones with  $N = 123$  and  $125$ .

N	$\nu_I$	Hg	Pb	Po	Ra	$\mu_{\text{Schmidt}}$
123	$(f_{5/2})^{-1}$	$\left\{ \begin{array}{l} \mu_I \ 0.84895(13)^{\text{a)}} \\ Q_S \ 0.40(4)^{\text{a)}} \end{array} \right.$	$\left\{ \begin{array}{l} 0.712(14)^{\text{b)}} \\ 0.14(3)^{\text{b)}} \end{array} \right.$	$\left\{ \begin{array}{l} 0.76(6)^{\text{c)}} \\ 0.28^{\text{a)}} \end{array} \right.$	0.90 0.45	1.37
125	$(p_{1/2})^{-1}$	$\mu_I \ 0.6010(1)^{\text{d)}}$	$0.592582(9)^{\text{a)}}$	-	0.62	0.638

a) ref [6], b) ref [10], c) ref [11], d) ref [9]

Figure captions

Fig. 1: Hyperfine structure in the ionic (RaII) and the atomic (RaI) resonance lines for  $^{223}\text{Ra}$ . The fluorescence signals are shown as a function of the acceleration voltage used for Doppler scanning.

Fig. 2: Positions of the observed resonances (even isotopes) and hyperfine structures (odd isotopes) with their centres of gravity (full dots) relative to  $^{214}\text{Ra}$ . Position and length of the horizontal lines represent position and relative height of the hfs components.

Fig. 3: Experimental magnetic dipole (circles) and electric quadrupole moments (dots) of the odd-A radium isotopes compared with the results from particle-rotor calculations. The vertical scale is given in n.m. and b, respectively. The main Nilsson orbital contributing to the nuclear wave functions is given at the top of the figure (assignment according to the Nilsson diagram in Appendix 41 of ref. [6]).

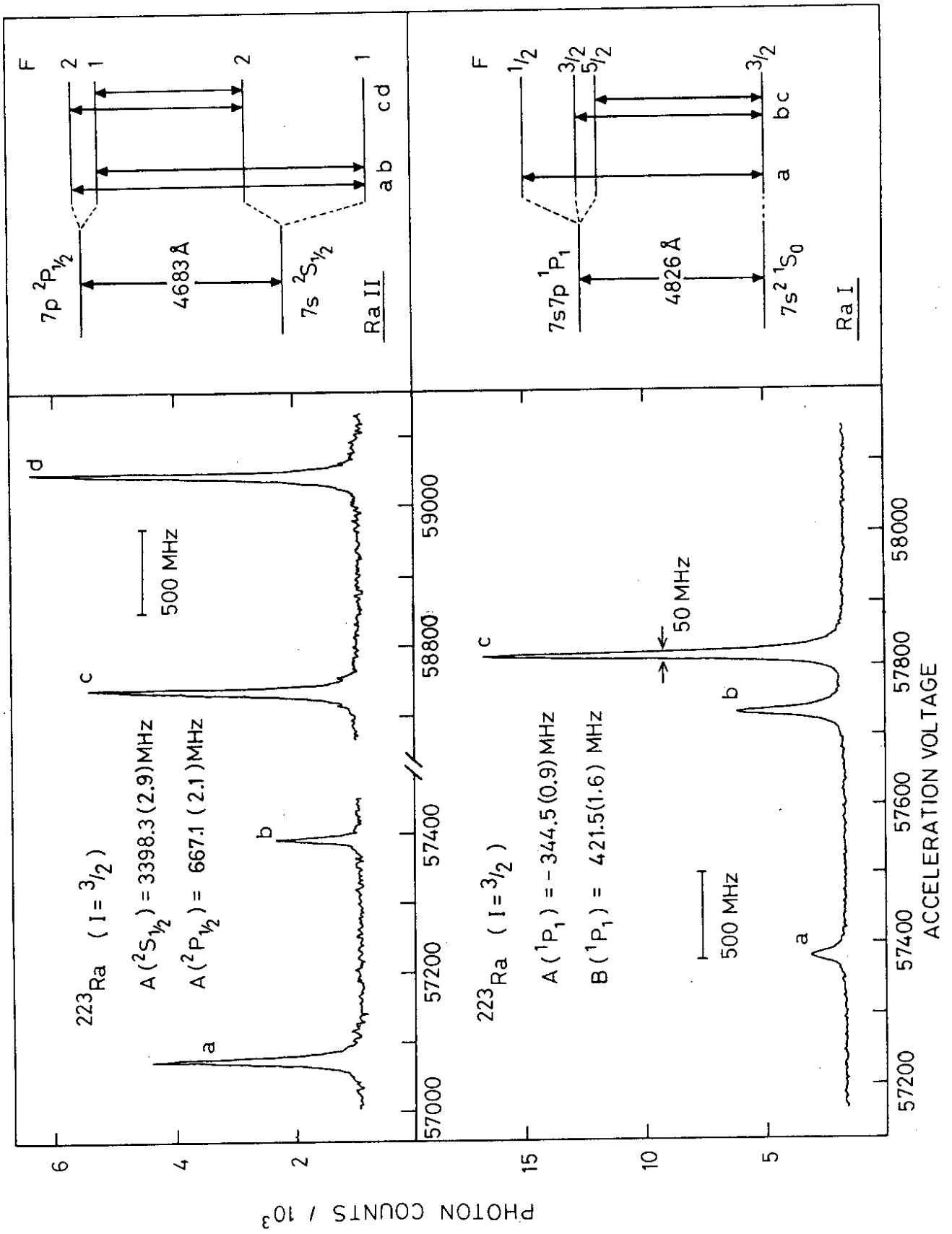


Fig. 1

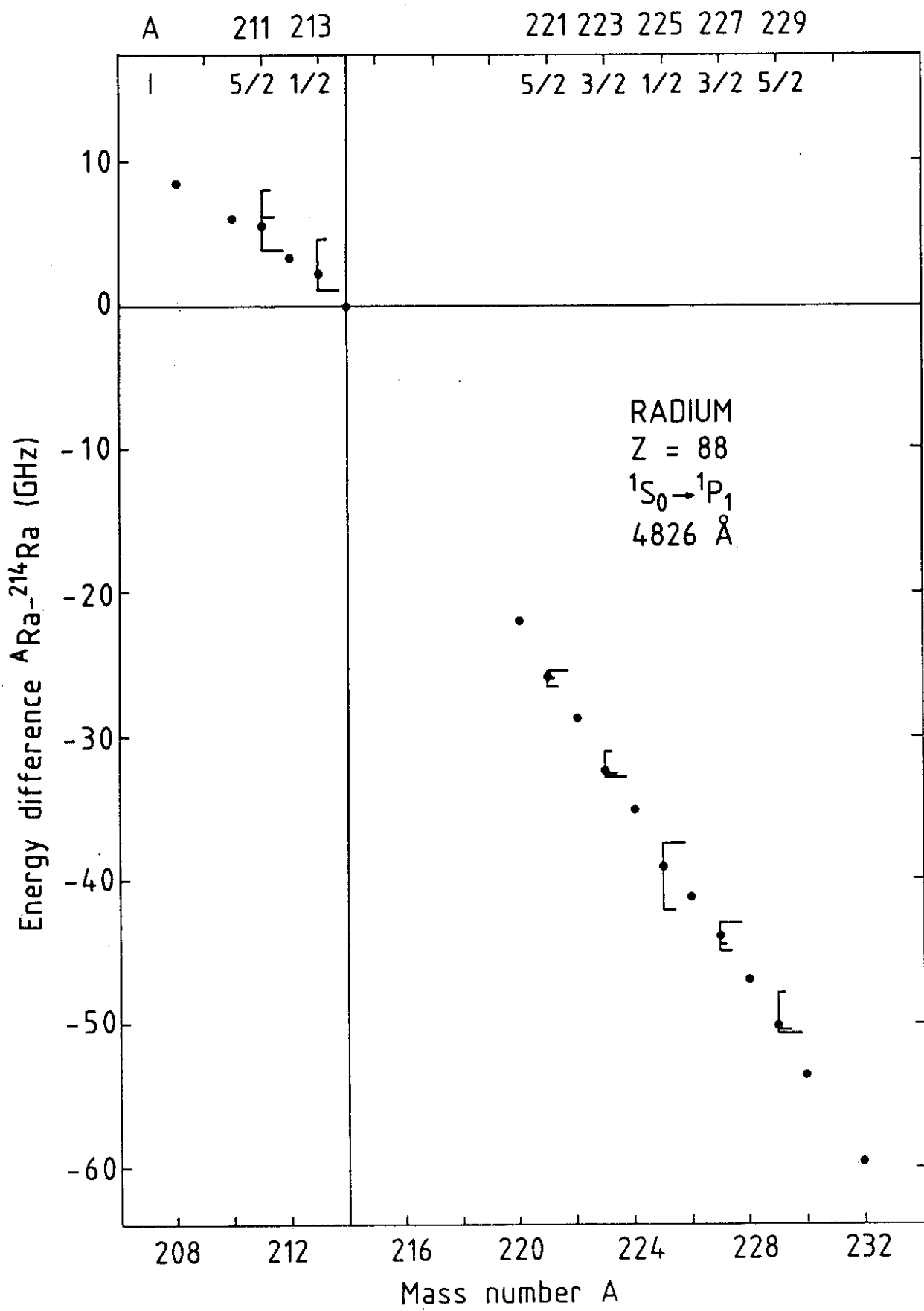


Fig. 2

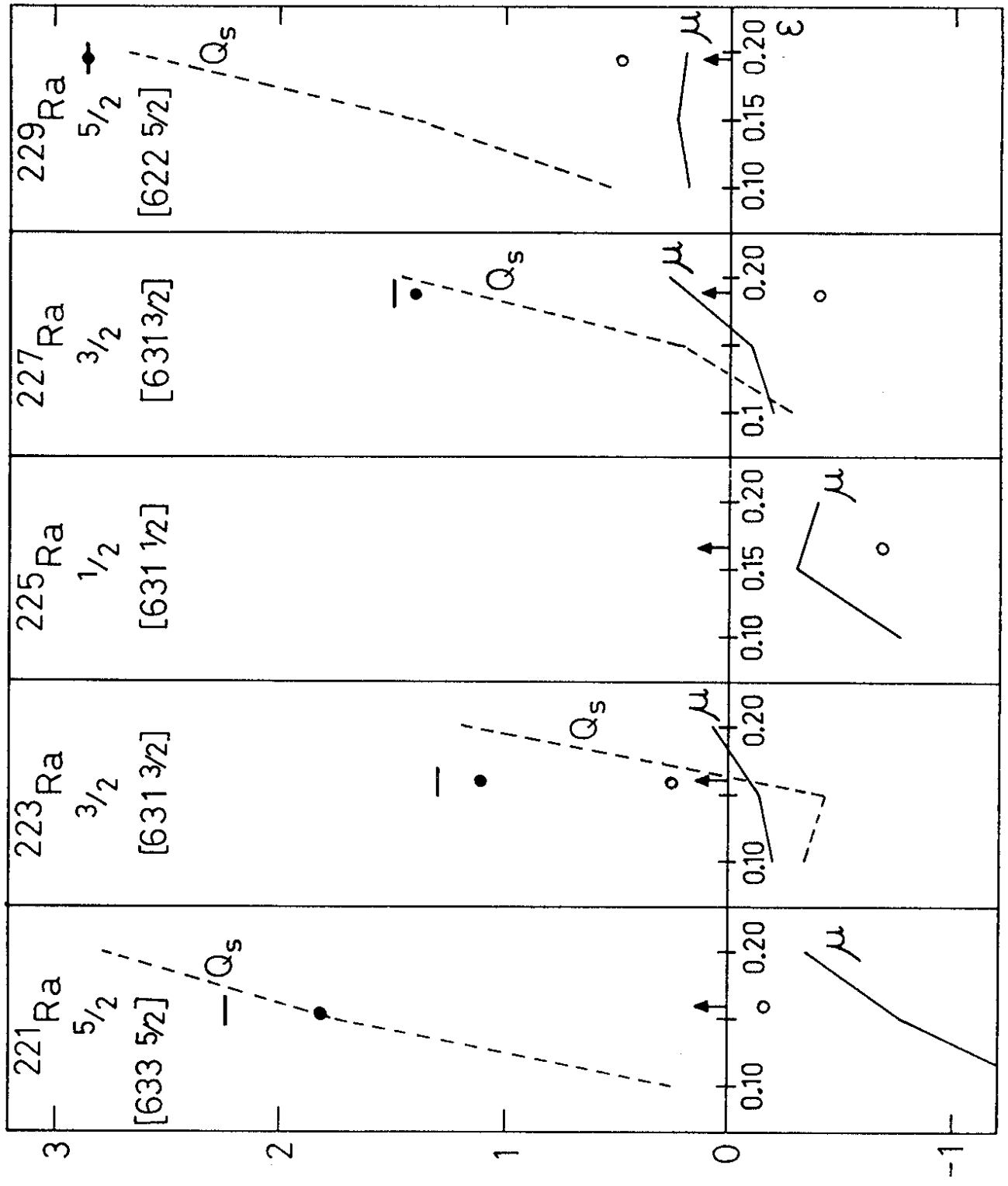


Fig. 3